JJMIE

Volume 18, Number 3, September. 2024
ISSN 1995-6665
Pages 509- 519
https://doi.org/10.59038/jjmie/180306
Editor-in-Chief: Prof. Ali M. Jawarneh

Jordan Journal of Mechanical and Industrial Engineering

Glass-Reinforced Aluminum Matrix Composite: Synthesizes, Analysis, and Hardness and Porosity Modeling Using Artificial Neural Networks

Ahmad Abu Sleem[1], Mazen Arafeh[1], Sameh Al-Shihabi[2], Ruba Obiedat[3], Yazan Al-Zain[*1]

[1]Industrial Engineering Department, University of Jordan, Amman, 11942, Jordan
[2]Industrial Engineering and Engineering Management Department, University of Sharjah, Sharjah, 27272, United Arab Emirates
[3]King Abdullah II School for Information Technology, The University of Jordan, Amman 11942, Jordan

Received 10 Mar 2024 Accepted 17 Jun 2024

Abstract

This study aims to investigate the predictive capabilities of artificial neural networks (ANNs) for Al-glass composites, specificallyin exploring the effect of glass particle size and content on hardness, porosity, and microstructure in Al-glass composites. Contents between 0-15 wt.% glass particles, with two size ranges— less than 53µm, and between 53-75µm— were incorporated within the pure aluminum matrix. Powder metallurgy was employed to produce the composite specimens. Pressing at 400 MPa was appliedto the powders to produce the green compacts. The sintering temperature was 550 °C. Three sintering periods were used: one, two, and four hours. The results indicate that the most significant factors affecting the hardness and porosity were glass percentage and sintering time. The highest hardness value of 27.50 HRB was obtained in specimen with 10% glass content sintered for 4 hours, with glass grain size of 53-75 µm. Whereas the highest porosity percentage of 5.4% was recorded for specimen with15% glass content sintered for 1 hour, with glass grain size of 53-75 µm. For ANN, three inputs and one output were established, where the Levenberg-Marquardt training algorithm neural network had the highest accuracy of prediction. With highest value of R2= 99.96% and 99.99%, and RMSE=0.06855 and 0.007141 for hardness and porosity, respectively. As such a high prediction accuracy was obtained using the ANNs, this study proves that ANN is a significant tools for the prediction of nonlinear relationships.

The novelty of this study lies in the combination of glass with aluminum as a new composite material, alongside the high predictive accuracy of the model with very small error margins, demonstrating the potential of ANNs to effectively handle nonlinear relationships in composite materials. Additionally, the ANN approach significantly saves time and costs associated with experimental testing and helps in finding the optimal combination with the best values of the mechanical properties, streamlining the development process for new composite materials.

Keywords: Artificial neural networks, Aluminum-Glass composites, Hardness, Porosity.

1. Introduction

Aluminum (Al) matrix composites (AMCs) are of paramount importance for several industries due to their desirable properties [1, 2]. For example, in the automobile industry, AMCs' high strength to weight ratio improves cars' efficiencies and reduces pollution [3]. In addition, AMCs are used in the fabrication of engine pistons and car brakes owing to their uniquethermal and wear resistance properties [2]. The properties of AMCs depend on several factors including the type, amount, shape, size, and distribution of the reinforcement within the matrix [4, 5]. Reinforcement materials include Al_2O_3 [6, 7], SiC [8, 9, 10], TiC [11], $ZrSiO_4$ [12], MgO [13], "SiC, Al_2O_3 and MgO" together [14], Cu [15], Mn and Cu [16], and Basalt [17]. A review of reinforcement material types and their effects on AMCs can be found elsewhere [18, 19].

In polymers, glass has been extensively used as a reinforcement material, enabling polymers to have outstanding mechanical and thermal properties [20]. In metals, for example, Patel et al. conducted a study on the effect of fly ash and e-glass addition on the properties of an Al6061 alloy [21]. The fly ashand e-glass were obtained from recycled electrical devices (e-waste). It was shown that the composite's compressive, tensile, and yield strengths were higher than those of the initial alloy. In the current work, powder metallurgy (PM) was used to reinforce Al with glass, while heat sinks and metallurgical synthesis were used by other researchers [22]. However, and up to the authors' knowledge, there is no systematic study on the

* Corresponding author e-mail: y.alzain@ju.edu.jo.

properties of the AMCs, which are reinforced with a normal window-type glass.

Hybrid metal matrix composites (HMMCs) are emerging as superior alternatives to traditional materials due to their enhanced metallurgical, mechanical, and tribological properties, making them viable for diverse manufacturing and construction applications [23]. The development of aluminum Al- and Mg-based HMMCs emphasizes their light weight, high strength, and wear resistance, suitable for engineering and medical applications, with stir casting recommended for effective fabrication [24]. In another work, the properties of Al7075-T6 based composites was optimized using SiC and MoS2 reinforcements through vacuum-assisted stir casting, achieving notable improvements in wear resistance and material dispersion, validated by advanced statistical and neural network models [25]. Additionally, the machinability of these composites has been enhanced, demonstrated by improved material removal rates and surface roughness in machining tests, supported by predictions from an artificial neural network, confirming the practical applicability and efficiency of HMMCs in industrial settings [26]. These studies collectively underline the potential of HMMCs to revolutionize material properties and machining processes, providing a foundation for future innovations in composite technology.

The following studies offer in-depth analyses on the development and optimization of MMCs, employing powder metallurgy and predictive modeling techniques. One study explores the properties of aluminum hybrid composites reinforced with micro SiC and nano ZrO2, utilizing both statistical methods and ANNs to assess the influence of reinforcement materials on wear behavior [27]. Another study focuses on predicting the properties of Cu-based composites reinforced with Al2O3 through a neural network, demonstrating the capacity of ANNs to manage complex property interactions effectively [28]. Furthermore, another study examines the enhancement of Al-based composites using rice husk ash, emphasizing improvements in mechanical properties and wear resistance, validated through ANN predictions [29].

Recent advancements in ANNs have significantly improved predictive modeling across various engineering applications, as evidenced in several studies. A study illustrates the application of a nonlinear neural Network Black-Box Model (NBBM) to predict the bending behavior of Ionic Polymer-Metal Composites (IPMCs) under variable conditions, demonstrating enhanced modeling capabilities without additional sensors [30]. Another study employs an ANN model to simulate the friction stir welding process of aluminum plates, optimizing parameters for mechanical property predictions with high accuracy [31]. In addition, a two-stage ANN effectively predicts shrinkage in composite material manufacturing, addressing complexities overlooked by conventional models [32]. Another study integrates a Multi-Objective Artificial Hummingbird Algorithm with ANN to optimize cutting conditions in machining polyoxymethylene (POM-C), leading to substantial improvements in material removal rates and machining efficiency [33]. Moreover, another study showcases the use of Particle Swarm Optimization to train an ANN for predicting Gas Metal Arc Welding parameters, surpassing traditional methods in flexibility, speed, and accuracy [34]. These studies collectively underscore the transformative impact of ANNs in engineering, offering robust, flexible, and precise solutions to complex industrial challenges.

In other related words, a study by Varol et al. discusses the use of ANNs to predict the physical and mechanical properties of Al2024-B4C composites, with particular attention to the impact of reinforcement size and content [35]. In another research, aluminum alloy composites reinforced with Al2O3 was studied, where ANNs successfully predicted the influence of compaction pressure and Al2O3 content on tensile strength and elongation [36]. In a different study, Shaikh addressed the tribological behavior of aluminum composites with silicon carbide and fly ash, identifying optimal fly ash content for minimal wear [37]. Moreover, a study by Varol et al. details the use of ANNs to predict the effects of manufacturing parameters on Al–Cu–Mg/B4Cp composites, achieving highly accurate predictions regarding density and porosity [38]. These studies collectively highlight the utility of advanced composites in improving material properties and optimizing manufacturing processes through experimental and predictive modeling approaches.

Understanding how the properties of a glass-reinforced AMCs change with the reinforcement process' inputs is crucial to attain the required properties. However, many costly experiments are required to fully understand the relation between glass, aluminum, and the synthesis process as inputs and the AMC's properties as outputs. Thus, in this study ANNs was employed to understand the nonlinear relationship between AMCs' inputs and outputs. When an ANN is adequately trained, it can perform predictions at high speed, and may be capable of detecting all possible interactions among inputs and process parameters. Therefore, ANNs were used by many researchers to predict materials properties [27, 39-45].

Many studies focus on the benefits of utilizing ANNs in prediction. For example, one such study explores the chemical composition of a new aluminum alloy, aiming to meet specific manufacturing and environmental standards. The ANN, trained on existing alloys, achieved a high accuracy of 99.33% correlation between its predictions and experimental results, demonstrating its potential to expedite the development of lightweight materials while reducing reliance on costly physical testing [46]. Another study shows the development of a novel methodology utilizing ANNs and the probabilistic Stu¨ssi fatigue S-N fields to create a constant life diagram (CLD) for predicting the

fatigue life of metallic materials under mean stress effects. By integrating experimental fatigue data and a multilayer perceptron network trained with the back-propagation algorithm, the study successfully estimates high-cycle fatigue regimes and suggests a method for calculating the fatigue resistance reduction factor, demonstrating strong alignment with experimental data [47].

For chemical-oriented, nonlinear systems, ANNs can model such systems with high accuracy [48]. Consequently, researchers have used ANNs to model and optimize the properties of several composites, such as plastic composites [49, 50] and AMCs [51, 52]. The accuracy of ANNs has exceeded 94% in modeling composites' properties as discussed by several researchers [28, 53-56]. We, therefore,

adopted the same approach and used ANNs to predict the glass-reinforced AMC's properties as a function of the glass properties and reinforcement process parameters.

2. Experimental procedure

In this section, specimen preparation steps and tests carried out is described. Testing both porosity and hardness is crucial for assessing material integrity, ensuring quality control, optimizing properties, and developing predictive models. High porosity often correlates with reduced hardness, indicating potential structural weaknesses that could impact performance under stress. This dual testing approach enables manufacturers to refine production processes to enhance the composite's mechanical properties, such as durability and load-bearing capacity. Additionally, correlating these parameters helps in predictive modeling and failure analysis, ensuring that the materials meet stringent standards for specific applications, thus improving overall design and functionality.

2.1. Specimen preparation

PM was used to produce the glass-reinforced AMC. Aluminum powder with the specifications of -325 mesh and 99.5% purity (trace metals basis) was used as a matrix material. As for glass powder, window plates were ground in a ball mill. After that, the glass was sieved using two sieves with opening sizes of 53μm and 75 μm. Thus, three powder size ranges were achieved: powders having grain size $<$ 53μm, between 53 μm and 75 μm, and grain size $>$ 75 μm. In this study, the first two size ranges were used. Table 1 showsthe glass constituents and their percentages (wt.%) as tested by the X-ray fluorescence (XRF) test.

Besides glass grain size, glass content in (wt.%) of the AMC is the second input variable that was consideredin this study. The three glass contents used are: 5%, 10 %, and 15%. Consequently, we hadsix different glass-reinforced AMCs for glass content and glassgrain size in addition to pure aluminum specimens. All specimens were cylindrical in shape and had a radius and a height of 31 mm and 4 mm, respectively. Figure 1 and Figure 2 show the mold used and the XRF powder press machine utilized for pressing the powders, respectively.

Al and glass powders were mixed for 60 minutes to ensure mixture homogeneity. After that, a pressure of 400 MPa was applied to the specimens. This pressure value was selected based on previous studies, where pressures between 240 MPa and 620 MPa were used [6, 12, 13, 57, 58]. After pressing, the green compacts were carefully collected and stored, as shown in Figure 3, to prevent any damage or contamination before sintering.

The third input variable in the experiment design was the sintering time. Sintering was performed using an electric furnace at 550 °C. Three sintering times were used; 1 hr, 2 hrs, and 4 hrs. Figure 4 shows the electric furnace used for sintering, ensuring precise temperature control. The various combinations of the glass grain size, glass content, and sintering time are shown in Table 2. It is worth noting that the last three specimens correspond to pure Al specimens (control samples). Once sintering was complete, the specimens were removed andimmediately stored in labeled transparent bags as illustrated in Figure 5.

Table 1. Window glass constituents and their composition

Constituents	Percentage %
SiO_2	97.033
Na_2O	1.79
CaO	0.45
K_2O	0.01
MgO	0.37
Al_2O_3	0.28
Fe_2O_3	0.007
TiO_2	0.06
SO_3	0

Figure 1. The mold of the XRF powder press machine.

Figure 2. XRF powder press machine.

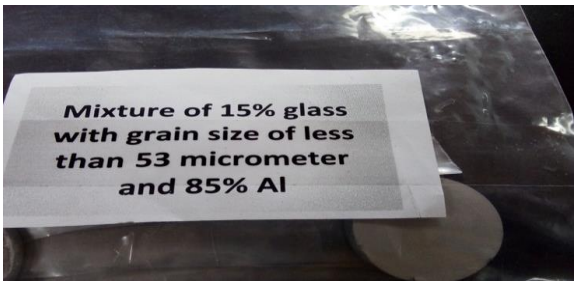

Figure 3. Storing of the green compacts.

  - Volume 18, Number 3 (ISSN 1995-6665)

Figure 4. Using electric furnace at 550 °C

2.2. Hardness testing

The two properties that were targeted in this study are hardnessand porosity. A Rockwell hardness testing machine was used to measure the hardness in Rockwell B scale (Hardness Rockwell B (HRB)) as shown in Figure 6. Results reported in this study show the averages of four readings. The effects of glass grain size, glass content, and sintering time are shown in Figure 7. It can be noticed that the hardness increases monotonically by increasing the sintering time for allspecimens except the pure aluminum specimens. The hardnessof the pure aluminum spacemen increased by increasing the sintering time up to 2 hours, then decreased slightly. It is suggested that grain overgrowth has taken place in the pure specimen after 2 hours of sintering.

Figure 5. Specimens removed and stored in labeled transparent bags

Figure 7(a) and Figure 7(b) show that the optimal glass percentage to maximize the specimens' harnesses is 10%. The second-best glass percentage value depended on the glass grain size. ComparingFigures 7a and 7b, we find that the second-best percentage is 5% for specimens having grain size between 53-75μm, whereas it is 15% for specimens having grain sizes $<$ 53μm. This nonlinear behavior justifies the use of ANN as discussed earlier.

2.3. Porosity testing

In this study, the porosity of 21 specimens was determined by first measuring the volume and mass of each specimen. The process involves the following steps:

1. **Volume Measurement:** The volume of each sample wascalculated based on its geometric dimensions.
2. **Mass Measurement:** Each sample was weighed in gramsusing a precise scale.

Figure 6. Rockwell hardness tester machine

Table 2. Various combinations of the glass grain size, glass content, and sintering time. [53,75] indicated grain size between 53 μm and 75 μm.

Combination	Glass (%)	Grain size (μm)	sintering (hr)
1	5	< 53	1
2	5	< 53	2
3	5	< 53	4
4	10	< 53	1
5	10	< 53	2
6	10	< 53	4
7	15	< 53	1
8	15	< 53	2
9	15	< 53	4
10	5	[53,75]	1
11	5	[53,75]	2
12	5	[53,75]	4
13	10	[53,75]	1
14	10	[53,75]	2
15	10	[53,75]	4
16	15	[53,75]	1
17	15	[53,75]	2
18	15	[53,75]	4
19	0	-	1
20	0	-	2
21	0	-	4

3. Density Calculation: The experimental density (ρexp) of the samples was computed using the formula:

$$\rho_{exp} = \frac{Mass}{Volume} \quad (1)$$

where Mass is in grams and Volume is in cubic centimeters.

4. **The theoretical density** of the glass-reinforced AMC, ρ, was calculated using Equation 2 where ρAl and ρglass represent the theoretical densities of the aluminum and glass, respectively. Moreover, %Al and %glass represent the percentages of aluminum and glass in the measured specimen.

$$\rho = \rho_{Al} \times \%Al + \rho_{glass} \times \%glass \quad (2)$$

5. **Comparison with Theoretical Density:** The experimental density was then compared to the theoretical density (ρth) known from literature:

$$Density\ Ratio = \frac{\rho_{exp}}{\rho_{th}} \quad (3)$$

6. **Porosity Calculation:** The porosity (P) was calculated using the density ratio, where a density ratio less than or equal 1 indicates the presence of porosity:

$$P = (1 - Density\ Ratio) \times 100\% \quad (4)$$

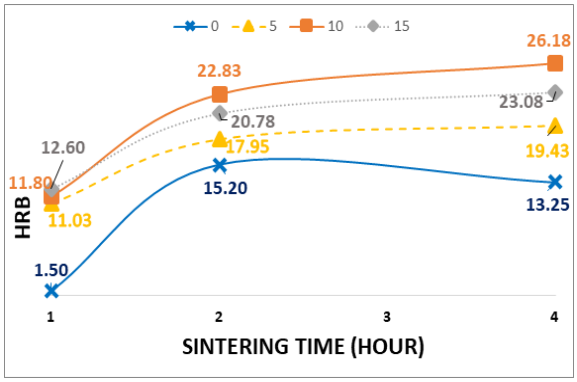

(a)

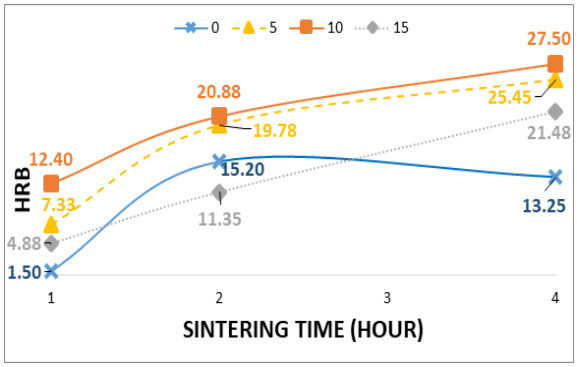

(b)

Figure 7. Effects of glass grain size, glass content, and sintering time on hardness. (a) Relationship between hardness and sintering time for different glasscontents for specimens having grain size < 53μm, and (b) Relationship between hardness and sintering time for different glass contents for specimens having grain size 53-75μm.

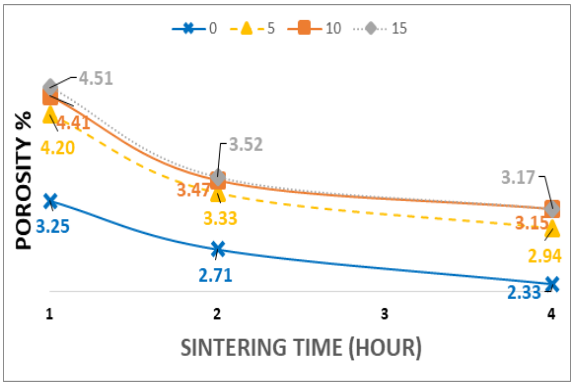

(a)

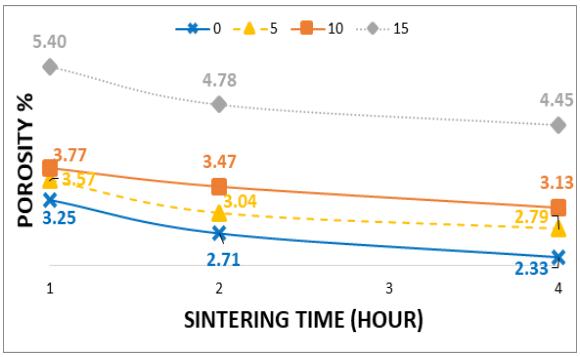

(b)

Figure 8. Effects of grain size, glass content, and sintering time on porosity. (a) Relationship between porosity and sintering time for different glass contents for specimens having grain size < 53μm and (b) Relationship between porosity and sintering time for different glasscontents for specimens having grain size 53-75μm.

For example, a density ratio of 0.9 results in a porosity of10%.

Unlike hardness, porosity decreases with the increase in sintering time, as shown in Figure 8. Figures 8a and 8b, show specimens having grain sizes < 53μm and between 53μm and 75μm, respectively. It is evident that the more the percentage of glass is,the higher the porosity is, for any sintering time and glass grainsize.

To ensure the reliability of our experimental results, each test was repeated four times for each sample, and each repetition was carried out on a different location. By using this approach,we aimed to mitigate any location-specific variables that could influence the results. After completing the tests, the average of the four outcomes for each sample was calculated. This method of averaging helps to smooth out any anomalies or variations that occurred due to external factors, providing a more reliable and consistent measure of the sample's behavior under test conditions.

3. ANN for modeling hardness and porosity

Modelling the relationship between the three inputs studied in this work and the two composite characteristics; hardness and porosity, is important to find the best inputs for any required application. Thus, in this section, the deep learning toolbox of Matlab was utilized to build an ANN model to predict the hardness and porosity of the glass-reinforced AMC. The best-found ANN model is then used to find the inputs needed to achieve the highest hardness.

3.1. ANN

In this study, the choice of ANNs as a soft computing technique was driven by ANNs' ability to model complex, nonlinear relationships inherent in material science, such as those between the components and properties of Al-glass composites. The performance of the ANN models not only confirms their suitability for accurately predicting mechanical properties but also demonstrates their potential to reduce the experimental workload and associated costs. This capability suggests broader implications for the field, where ANNs can be utilized to optimize material properties in the design phase leading to innovative developments in composite manufacturing and a faster transition from laboratory testing to practical application.

Two different ANNs were built and trained, one to predict hardness and another one to predict porosity. The deep learning toolbox has different ANN training algorithms. Matlab users can choose different network configurations. The Configuration identifies the number of hidden layers, number of neurons,and activation functions used in the neurons. Thus, fourteen different training algorithms and structures were investigated to model the relationship between the experiments' inputs and each targeted output. Lastly, to build and test the different ANNs, the data were divided into 70% for training, 15% for validation, and 15% for testing.

To find the best ANN model, the following algorithms were tested:

1. Bayesian regulation (BR),
2. BFGS quasi-newton (BFG),
3. Conjugate gradient with beale-powll restarts (CGB),
4. Conjugate gradient backpropagation with fletcher-reevesrestarts (CGF),
5. Conjugate gradient with polka-ribiere restarts (CGP),
6. Gradient decent (GD),
7. Gradient descent with momentum (GDM),
8. Gradient descent with adaptive learning rate (GDA),
9. Gradient descent with momentum and adaptive LR (GDX),
10. Levenberg-marquardt (LM),
11. One step secant (OSS),
12. Random weight/bias rule (R)
13. Rprop (RP)
14. Scaled conjugate gradient (SCG)

Two configurations were considered for the number of hidden layers and neurons after exploring many architectures with 3, 4, and 5 hidden layers. It was discovered that configurations with 1 and 2 hidden layers yielded more accurate results. As forthe neurons, multiple configurations were tested, and the mosteffective number of neurons that consistently produced the bestaccuracy were approximately 84 for the one-layer model and 21 foreach layer in the two-layers model. Roman numerals were used to denote these two configurations, such that configuration I is forthe one-layer model while configuration II is for the two-layer model. Lastly, two different selections for the activation functions used by the neurons were tested. For configuration I, the test was at first for selection one that uses the hyperbolic tangent sigmoid transfer function (transig) and then for selection two that uses the standard sigmoid transfer function (logsig). For the two-hidden layers configuration, configuration II, selection 1 uses tansig for all the neurons while selection 2 uses tansig in the first layer and logsig in the second layer. The output neuron uses a tansig function, except for selection 2 of configuration 1 that uses logsig activation functions in the hidden layer. Thus, a total of 56 different ANNs were accomplished from this experiment.

Henceforth, we denote the different ANN models using a three-letter notation A-B-C where A, B, and C represent the training algorithm, network configuration, and activation function selection. For example, an ANN model indicated by CGF-II-1 means that a CGF algorithm is used to train a network having the second configuration, i.e., it has two hidden layers and 21 neurons in each layer, and the activation functions follow selection 1 that uses tansig activation function. The different ANNs were compared using two measures, the coefficient of determination R^2, as shown in Equation 5, and the root mean square error (RMSE), as shown in Equation 6. 1000 epochs were used to train each ANN configuration.

$$R^2 = 1 - \sqrt{\frac{\sum_{i=1}^{n}(y_i - \hat{y}_i)^2}{\sum_{i=1}^{n}(y_i - \bar{y})^2}} \quad (5)$$

$$RMSE = \sqrt{\frac{1}{n}\sum_{i=1}^{n}(y_i - \hat{y}_i)^2} \quad (6)$$

Table 3 show the R^2 and RMSE values obtained by the 56 ANN models. Moreover, Figure 9 shows the values of the R^2 measure for hardness and porosity prediction for the 56 ANN models. From Table 3 and Figure 9, it is clear that the ANN model LM-I-1 is the best model to predict hardness and porosity.

3.2. Optimal hardness and validation

LM-I-1 ANN model were used to have the highest hardness and the corresponding inputs. The LM-I-1 model predicted thehighest hardness value to be 27.57119 HRB for a specimen sintered for 5 hours and 20 minutes and contained 14% glass with particle size range of 53-75µm. Thus, we validate our model byfabricating a real specimen having the specifications mentioned above. The average hardness of the fabricated sample was ~27.6 HRB, which is similar to the hardness predicted by the proposed model.

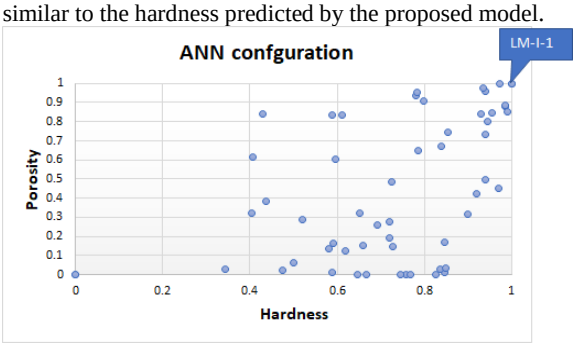

Figure 9. Hardness and porosity prediction accuracy measured using R^2 for the 56 ANN models

4. Analysis

In this section, the results are thoroughly explained. First, the hardness results were discussed, then the porosity results. In this study, quantitative data were collected under controlled laboratory conditions. Porosity was measured through volume and density principles, while hardness was assessed using Rockwell hardness tester machine. Data was recorded in structured spreadsheets, with each entry detailing sample name, porosity, and hardness values, alongside calibration and testing conditions. Instruments were regularly recalibrated, and error handling included consistency checks.

4.1. Hardness

To investigate the effect of glass content on the grain size, SEM images were captured using the Quanta 600 device (shown in Figure 10) for specimens with different glass content and sintering times. An example is shown in Figure 11. Here, the formation of grains is obvious in all samples tested. In addition, and as previously shown in Figure 8, the grain size decreased slightly on increasing the glass content. It is believed that the precipitates (glass particles) act as nucleationsites for the formation of new grains. In addition, such precipitates hinder the movement of grain boundaries hence leading to a refined structure.

Figure 12 shows the effects of the glass content and sintering time on the grain sizes of the specimens having a glass grain size less than 53μm. Also, it shows that the grain size increases when increasing the sintering period but decreases when increasing the proportion of glass.

4.2. Porosity

The addition of glass particles to the Al matrix caused internal stress and lattice defects such as phase boundaries. This glass addition has led to an increase in porosity, which explains the results discussed earlier and summarized in Figure 8. The increase in hardness can be attributed to the glass ability to minimize the plastic flow in the matrix. Thus, the larger the glass grain size within the composite matrix, the higher the hardness value.

5. Conclusions and future research

In this study, the effects of glass content on a glass-reinforced AMC were investigated. In addition, the effects of the glass and sintering time on the hardness and porosity of the resulting AMC was modeled. The paper ends by justifying the behavior of the composite using an SEM.

The highest hardness was obtained for a specimen having 10% glass of size 53-75μm that was sintered for four hours. Moreover, the highest porosity value was obtained for a specimen having the same grain size; however, it has a glass content of 15% and was sintered for one hour. The SEM micrographs showed that when increasing the sintering time, the grain size became larger, but the grain size became smaller when increasing the glass percentage. The glass content and the resulting grain sizes after sintering have affected the AMC as follow: (1) hardness increased due to the ability of the glass to minimize the plastic flow of the matrix; (2) porosity increased because the glass resulted in stresses and lattice defect, e.g., phase boundaries.

Because of the expenses of creating and testing the glass-reinforced AMC specimens and the nonlinear relationship between the specimens' inputs and outputs, we tested 56 different ANN configurations to model these nonlinear relationships. Where the Levenberg-Marquardt training algorithm neural network and has one layer having 84 neurons where the activation function is a tansig had the highest accuracy of prediction, with values of R2= 99.96% and 99.99%, and RMSE=0.06855 and 0.007141 for hardness and porosity, respectively. With the ANNs obtaining such high prediction accuracy, it shows that they are significant tools for the prediction of nonlinear relationships.

The application of the Al-glass composites is primarily in industries where high strength-to-weight ratios are crucial, such as aerospace, automotive, and military sectors. These composites offer enhanced mechanical properties, including improved hardness and reduced porosity, making them ideal for structural components that require both lightness and durability.

In future research, the effect of other glass grain size ranges, sintering times, or glass contents may be tested. Furthermore, a different reinforcement material, or a mixture of different reinforcement materials, can be tested. Other mechanical properties can also be tested, like compressive strength, impact, and elongation.

Figure 10. Quanta 600 device.

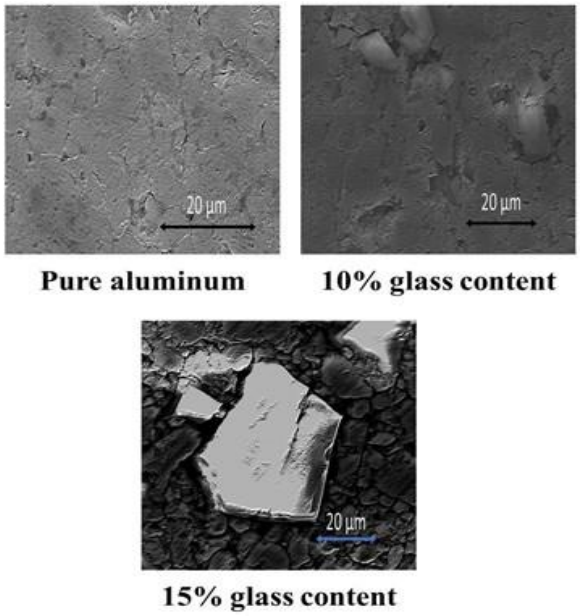

Figure 11. Comparison between three specimens, pure aluminum, 10% glass content, and 15% glass content, that were sintered for 2 hours

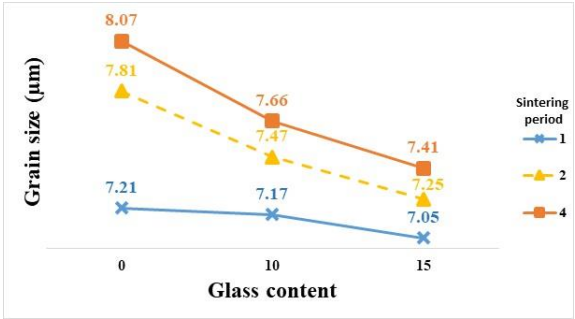

Figure 12. The effect of glass content and sintering period on the grain size of specimens with grain size rang less than 53μm

Table 3. Different ANN configurations and the resulting hardness and porosity accuracy estimates

ANN	Hardness		Porosity		ANN	Hardness		Porosity	
	R^2	RMSE	R^2	RMSE		R^2	RMSE	R^2	RMSE
BR-I-1	0.62	3.06	0.13	0.60	GDA-I-1	0.85	2.08	0.04	0.76
BR-I-2	0.69	2.27	0.26	0.70	GDA-I-2	0.73	2.16	0.15	0.70
BR-II-1	0.65	1.99	0.00	0.64	GDA-II-1	0.78	1.57	0.94	0.17
BR-II-2	0.58	3.33	0.14	0.65	GDA-II-2	0.61	2.17	0.83	0.31
BFG-I-1	0.52	3.95	0.29	0.76	GDX-I-1	0.66	3.28	0.15	0.66
BFG-I-2	0.00	3.35	0.00	56.10	GDX-I-2	0.34	2.81	0.03	0.70
BFG-II-1	0.72	1.87	0.28	0.57	GDX-II-1	0.97	0.59	0.45	0.48
BFG-II-2	0.83	1.52	0.00	50.10	GDX-II-2	0.59	2.20	0.84	0.27
CGB-I-1	0.85	1.36	0.01	50.10	LM-I-1	1.00	0.07	1.00	0.01
CGB-I-2	0.67	2.30	0.00	56.10	LM-I-2	0.72	2.12	0.49	0.64
CGB-II-1	0.78	1.64	0.65	0.38	LM-II-1	1.00	0.08	1.00	0.01
CGB-II-2	0.41	2.96	0.62	0.41	LM-II-2	0.97	0.60	1.00	0.04
CGF-I-1	0.94	0.82	0.96	0.13	OSS-I-1	0.72	3.32	0.19	0.82
CGF-I-2	0.76	2.11	0.00	0.70	OSS-I-2	0.00	3.35	0.00	0.70
CGF-II-1	0.43	2.84	0.84	0.26	OS-II-1	0.94	0.82	0.49	0.58
CGF-II-2	0.80	1.53	0.91	0.19	OS-II-2	0.93	0.88	0.84	0.26
CGP-I-1	0.99	0.39	0.88	0.22	R-I-1	0.78	3.46	0.95	0.14
CGP-I-2	0.74	2.11	0.00	0.70	R-I-2	0.85	2.04	0.17	0.69
CGP-II-1	0.93	0.90	0.98	0.10	R-II-1	0.99	0.38	0.85	0.25
CGP-II-2	0.94	0.83	0.73	0.34	R-II-2	0.98	0.44	0.89	0.22
GD-I-1	0.77	3.21	0.00	50.74	RP-I-1	0.85	1.97	0.75	0.51
GD-I-2	0.59	2.32	0.01	0.71	RP-I-2	0.59	2.46	0.17	0.69
GD-II-1	0.84	1.88	0.03	0.76	RP-II-1	0.96	0.78	0.85	0.26
GD-II-2	0.65	3.17	0.32	0.53	RP-II-2	0.90	1.25	0.32	0.64
GDM-I-1	0.60	3.50	0.61	0.41	SCG-I-1	0.92	1.22	0.43	0.53
GDM-I-2	0.47	2.50	0.03	0.71	SCG-I-2	0.50	2.44	0.06	0.70
GDM-II-1	0.44	2.82	0.39	0.50	SCG-II-1	0.94	0.80	0.80	0.29
GDM-II-2	0.40	2.92	0.32	0.54	SCG-II-2	0.84	1.36	0.67	0.37

6. Recommendations and limitations

6.1. Recommendations

15. **Integration of Other Modeling Techniques:** Combine artificial neural networks (ANNs) with other machine learning or computational methods, such as genetic algorithms or fuzzy logic, to enhance the prediction models and possibly improve accuracy and generalizability.
16. **Real-world Application Testing:** Pilot the use of the developed composites in real-world applications, such as inautomotive or aerospace components, to validate the laboratory findings in operational environments.
17. **Longitudinal Studies:** Conduct long-term studies to assess the durability and lifespan of the composites under various operational stresses, providing data that could improve future design and manufacturing processes.

6.2. Limitations

18. **Generalizability of ANN Models:** While artificial neural networks (ANNs) showed high predictive accuracy withinthe tested configurations, these models might not generalize well to other types of composites or different conditions without retraining.
19. **Scale of Production:** The findings are based on laboratory-scale experiments. Scaling up to industrial production might introduce new variables that were not accounted for in the study.
20. **Dependency on Quality of Data:** The accuracy of ANN predictions is highly dependent on the quality and range of the input data. Any limitations in data variability or measurement accuracy can significantly affect the model'sperformance.

7. The key findings

21. Analysis determined that the most influential factors on hardness and porosity were the percentage of glass and the duration of sintering.
22. The highest recorded hardness value was 27.50 HRB, achieved in specimens with 10% glass content sintered for four hours with a grain size of 53-75 μm.
23. The maximum porosity observed was 5.4%, in specimens containing 15% glass content and sintered for one hour, also with a grain size of 53-75 μm.
24. Three input variables and one output were modeled using artificial neural networks (ANNs), which employed the Levenberg-Marquardt training algorithm, achieving high prediction accuracy with R^2 values of 99.96% and 99.99%, and RMSE values of 0.06855 and 0.007141 for hardness and porosity, respectively.
25. The success of the ANNs demonstrates their capacity as effective tools for predicting nonlinear relationships in material science, indicating significant time and cost savings in experimental testing.
26. The study highlights the ANN's role in identifying the optimal combinations of mechanical characteristics, enhancing the efficiency of developing new composite materials.

8. Data Availability

All data required to duplicate the experiment of can be downloaded from https://github.com/ samehShihabi/ANN-for-glass- reinforced-AMC.

References

[1] N. Fatchurrohman, I. Iskandar, S. Suraya, K. Johan, "Sustainable analysis in the product development of Al-metal matrix composites automotive component," Applied Mechanics and Materials, Vol. 695, 2015, pp. 32–35. https://doi.org/10.4028/www.scientific.net/AMM.695.32.

[2] S. T. Mavhungu, E. T. Akinlabi, M. A. Onitiri, F. M. Varachia, "Aluminum matrix composites for industrial use: advances and trends," Procedia Manufacturing, Vol. 7, 2017, pp. 178–182. https://doi.org/10.1016/j.promfg.2016.12.045.

[3] A. Macke, B. F. Schultz, P. Rohatgi, "Metal matrix composites," Adv. Mater. Processes, Vol. 170, No. 3, 2012, pp. 19–23. https://doi.org/10.31399/asm.amp.2012-03.p019.

[4] M. N. Mazlee, J. B. Shamsul, Y. Zamri, "Fabrication and dynamic mechanical properties of A357-stainless steel composites."

[5] B. Venkatesh, B. Harish, "Mechanical properties of metal matrix composites (Al/SiCp) particles produced by powder metallurgy," International Journal of Engineering Research and General Science, Vol. 3, No. 1, 2015, pp. 1277–1284.

[6] M. Rahimian, N. Parvin, N. Ehsani, "Investigation of particle size and amount of alumina on microstructure and mechanical properties of Al matrix composite made by powder metallurgy," Materials Science and Engineering: A, Vol. 527, Nos. 4-5, 2010, pp. 1031–1038. https://doi.org/10.1016/j.msea.2009.09.034.

[7] M. Rahimian, N. Parvin, N. Ehsani, "The effect of production parameters on microstructure and wear resistance of powder metallurgy Al–Al2O3 composite," Materials & Design, Vol. 32, No. 2, 2011, pp. 1031–1038. https://doi.org/10.1016/j.matdes.2010.07.016.

[8] O. El-Kady, A. Fathy, "Effect of SiC particle size on the physical and mechanical properties of extruded Al matrix nanocomposites," Materials & Design (1980-2015), Vol. 54, 2014, pp. 348–353. https://doi.org/10.1016/j.matdes.2013.08.049.

[9] V. Umasankar, M. A. Xavior, S. Karthikeyan, "Experimental evaluation of the influence of processing parameters on the mechanical properties of SiC particle reinforced AA6061 aluminum alloy matrix composite by powder processing," Journal of Alloys and Compounds, Vol. 582, 2014, pp. 380–386. https://doi.org/10.1016/j.jallcom.2013.07.129.

[10] S. P. Dwivedi, R. Sahu, "Effects of SiC Particles Parameters on the Corrosion Protection of Aluminum-based Metal Matrix Composites using Response Surface Methodology," Jordan Journal of Mechanical and Industrial Engineering, Vol. 12, No. 4, 2018.

[11] M. Ali, S. Falih, "Synthesis and Characterization of Aluminum Composites Materials Reinforced with TiC Nano-Particles," Jordan Journal of Mechanical and Industrial Engineering, Vol. 8, No. 5, 2014.

[12] H. Abdizadeh, M. Ashuri, P. T. Moghadam, A. Nouribahadory, H. R. Baharvandi, "Improvement in physical and mechanical properties of aluminum/zircon composites fabricated by powder metallurgy method," Materials & Design, Vol. 32, Nos. 8-9, 2011, pp. 4417–4423. https://doi.org/10.1016/j.matdes.2011.03.071.

[13] M. A. Baghchesara, H. Abdizadeh, "Microstructural and mechanical properties of nanometric magnesium oxide particulate-reinforced aluminum matrix composites produced by powder metallurgy method," Journal of Mechanical Science and Technology, Vol. 26, 2012, pp. 367–372. https://doi.org/10.1007/s12206-011-1101-9.

[14] A. R. I. Kheder, G. S. Marahleh, D. M. K. Al-Jamea, "Strengthening of Aluminum by SiC, Al2O3 and MgO," Jordan Journal of Mechanical and Industrial Engineering, Vol. 5, No. 6, 2011.

[15] N. Alshabatat, S. Al-qawabah, "Effect of 4% wt. Cu Addition on the Mechanical Characteristics and Fatigue Life of Commercially Pure Aluminum," Jordan Journal of Mechanical and Industrial Engineering, Vol. 9, No. 4, 2015.

[16] L. M. Shehadeh, I. S. Jalham, "The Effect of Adding Different Percentages of Manganese (Mn) and Copper (Cu) on the Mechanical Behavior of Aluminum," Jordan Journal of Mechanical and Industrial Engineering, Vol. 10, No. 1, 2016.

[17] C. B. Abraham, V. B. Nathan, S. R. Jaipaul, D. Nijesh, M. Manoj, S. Navaneeth, "Basalt fibre reinforced aluminium matrix composites–a review," Materials Today: Proceedings, Vol. 21, 2020, pp. 380–383. https://doi.org/10.1016/j.matpr.2019.06.135.

[18] S. Arunkumar, M. S. Sundaram, S. Vigneshwara, "A review on aluminium matrix composite with various reinforcement particles and their behaviour," Materials Today: Proceedings, Vol. 33, 2020, pp. 484–490. https://doi.org/10.1016/j.matpr.2020.05.053.

[19] P. Samal, P. R. Vundavilli, A. Meher, M. M. Mahapatra, "Recent progress in aluminum metal matrix composites: A review on processing, mechanical and wear properties," Journal of Manufacturing Processes, Vol. 59, 2020, pp. 131–152. https://doi.org/10.1016/j.jmapro.2020.09.010.

[20] A. Gnanavelbabu, P. Saravanan, K. Rajkumar, P. Sabarinathan, S. Karthikeyan, "Mechanical strengthening effect by various forms and orientation of glass fibre reinforced isopthalic polyester polymer composite," Materials Today: Proceedings, Vol. 5, No. 13, 2018, pp. 26850–26859. https://doi.org/10.1016/j.matpr.2018.08.167.

[21] S. Patel, R. S. Rana, S. K. Singh, "Study on mechanical properties of environment friendly Aluminium E-waste Composite with Fly ash and E-glass fiber," Materials Today: Proceedings, Vol. 4, No. 2, 2017, pp. 3441–3450. https://doi.org/10.1016/j.matpr.2017.02.233.

[22] M. Zasadzin´ska, P. Strzepek, A. Mamala, P. Noga, "Reinforcement of aluminium-matrix composites with glass fibre by metallurgical synthesis," Materials, Vol. 13, No. 23, 2020, p. 5441. https://doi.org/10.3390/ma13235441.

[23] N. Singh, R. M. Belokar, R. S. Walia, "A critical review on advanced reinforcements and base materials on hybrid metal matrix composites," Silicon, 2020, pp. 1–24. https://doi.org/10.1007/s12633-020-00853-z.

[24] N. Singh, R. M. Belokar, "Tribological behavior of aluminum and magnesium-based hybrid metal matrix composites: A state-of-art review," Materials Today: Proceedings, Vol. 44, 2021, pp. 460–466. https://doi.org/10.1016/j.matpr. 2020.09.757.

[25] N. Singh, D. Deepika, "Empirical investigation on controlled porosity level and dry sliding wear behavior of Al7075-(T6) doped with SiC+ MoS2 based hybrid composites via advanced vacuum-assisted stir casting," Proceedings of the Institution of Mechanical Engineers, Part C: Journal of Mechanical Engineering Science, 2024, p. 09544062241228973. https://doi.org/10.1177/09544062241228973.

[26] N. Singh, D. Deepika, R. M. Belokar, R. S. Walia, "Experimental probe on machining attributes of Al 7075-T6/SiC/crumb rubber/MoS_2-based green hybrid composite using artificial neural network model," Proceedings of the Institution of Mechanical Engineers, Part E: Journal of Process Mechanical Engineering, Vol. 237, No. 5, 2023, pp. 1643–1652. https://doi.org/10.1177/09544089221122071.

[27] S. Arif, M. T. Alam, A. H. Ansari, M. B. N. Shaikh, M. A. Siddiqui, "Analysis of tribological behaviour of zirconia reinforced Al-SiC hybrid composites using statistical and artificial neural network technique," Materials Research Express, Vol. 5, No. 5, 2018, 056506. https://doi.org/10. 1088/2053-1591/aabec8.

[28] M. Amirjan, H. Khorsand, M. H. Siadati, R. E. Farsani, "Artificial Neural Network prediction of Cu–Al_2O_3 composite properties prepared by powder metallurgy method," Journal of Materials Research and Technology, Vol. 2, No. 4, 2013, pp. 351–355. https://doi.org/10.1016/j.jmrt.2013.08.001.

[29] M. B. N. Shaikh, S. Raja, M. Ahmed, M. Zubair, A. Khan, M. Ali, "Rice husk ash reinforced aluminium matrix composites: fabrication, characterization, statistical analysis and artificial neural network modelling," Materials Research Express, Vol. 6, No. 5, 2019, p. 056518. https://doi.org/10.1088/2053-1591/aafbe2.

[30] B. Kazem, J. Khawwaf, "Estimation Bending Deflection in an Ionic Polymer Metal Composite (IPMC) Material using an Artificial Neural Network Model," Jordan Journal of Mechanical and Industrial Engineering, Vol. 10, No. 2, 2016.

[31] Y. K. Yousif, K. M. Daws, B. I. Kazem, "Prediction of friction stir welding characteristic using neural network," Jordan Journal of Mechanical and Industrial Engineering, Vol. 2, No. 3, 2008, pp. 151–155.

[32] I. Jalham, "A Two-stage Artificial Neural Network Model to Predict the Shrinkage of a Polystyrene Matrix Reinforced with Silica Sand and Cement," Jordan Journal of Mechanical and Industrial Engineering, Vol. 5, No. 3, 2011.

[33] T. Hakmi, A. Hamdi, A. Laouissi, H. Abderazek, S. Chihaoui, M. A. Yallese, "Mathematical Modeling Using ANN Based on k-fold Cross Validation Approach and MOAHA Multi-Objective Optimization Algorithm During Turning of Polyoxymethylene POM-C," Jordan Journal of Mechanical and Industrial Engineering, Vol. 81, No. 1, 2024.

[34] P. Sreeraj, T. Kannan, S. Maji, "PSO-Based Neural Network Prediction and its Utilization in GMAW Process," Jordan Journal of Mechanical and Industrial Engineering, Vol. 8, No. 5, 2014.

[35] T. Varol, A. Canakci, S. Ozsahin, "Artificial neural network modeling to effect of reinforcement properties on the physical and mechanical properties of Al2024–B4C composites produced by powder metallurgy," Composites Part B: Engineering, Vol. 54, 2013, pp. 224–233. https://doi.org/10. 1016/ j.compositesb.2013.05.015.

[36] M. Mohsin, M. A. Qazi, M. Suhaib, M. B. N. Shaikh, M. Misbah, "Analysis and prediction of the tensile strength of aluminum alloy composite using statistical and artificial neural network technique," Engineering Research Express, Vol. 3, No. 1, 2021, p. 015002. https://doi.org/10.1088/2631-8695/abd4f1.

[37] M. N. Shaikh, "A statistical analysis of wear behavior of fly ash reinforced Al-Sic hybrid composites," J Powder Metall Min, Vol. 7, 2018, pp. 190–194.

[38] T. Varol, A. Canakci, S. Ozsahin, "Modeling of the Prediction of densification behavior of powder metallurgy Al–Cu–Mg/B4C composites using artificial neural networks," Acta Metallurgica Sinica (English Letters), Vol. 28, 2015, pp. 182–195. https://doi.org/10.1007/s40195- 014-0184-6.

[39] N. Altinkok, R. Koker, "Neural network approach to prediction of bending strength and hardening behaviour of particulate reinforced (Al–Si–Mg)-aluminium matrix composites," Materials & Design, Vol. 25, No. 7, 2004, pp. 595–602. https://doi.org/10.1016/j.matdes.2004.02.014.

[40] N. Altinkok, R. Koker, "Use of artificial neural network for prediction of physical properties and tensile strengths in particle reinforced aluminum matrix composites," Journal of Materials Science, Vol. 40, No. 7, 2005, pp. 1767– 1770.

[41] O¨.Erkan,B.Is ¸ık,A.C ¸ic ¸ek,F.Kara,Prediction of damage factor in end milling of glass fibre reinforced plastic composites using artificial neural network," Applied Composite Materials, Vol. 20, 2013, pp. 517–536.

[42] T. Varol, A. Canakci, S. Ozsahin, "Prediction of the influence of processing parameters on synthesis of Al2024- B4C composite powders in a planetary mill using an artificial neural network," Science and Engineering of Composite Materials, Vol. 21, No. 3, 2014, pp. 411–420. https://doi.org/10.1515/ secm-2013-0148.

[43] G. Chen, H. Wang, A. Bezold, C. Broeckmann, D. Weichert, L. Zhang, "Strengths prediction of particulate reinforced metal matrix composites (PRMMCs) using direct method and artificial neural network," Composite Structures, Vol. 223, 2019, p. 110951. https://doi.org/10.1016/j.compstruct. 2019.110951.

[44] U. Devadiga, R. K. R. Poojary, P. Fernandes, "Artificial neural network technique to predict the properties of multiwall carbon nanotube-fly ash reinforced aluminium composite," Journal of Materials Research and Technology, Vol. 8, No. 5, 2019, pp. 3970–3977. https://doi.org/10.1016/j.jmrt. 2019.07.005.

[45] S. Ponnuvel, N. Senthilkumar, "A study on machinability evaluation of Al-Gr-B4C MMC using response surface methodology-based desirability analysis and artificial neural network technique," International Journal of Rapid Manufacturing, Vol. 8, Nos. 1-2, 2019, pp. 95–122. https://doi.org/10.1504/IJRAPIDM.2019.097030.

[46] M. Jimenez-Martinez, M. Alfaro-Ponce, C. Mun˜oz- Iban˜ez, "Design of an Aluminum Alloy Using a Neural Network-Based Model," Metals, Vol. 12, No. 10, 2022, p. 1587. https://doi.org/10.3390/met12101587.

[47] J. F. Barbosa, J. A. Correia, R. F. Ju´nior, A. M. De Jesus, "Fatigue life prediction of metallic materials considering mean stress effects by means of an artificial neural network," International Journal of Fatigue, Vol. 135, 2020, p. 105527. https://doi.org/10.1016/j.ijfatigue.2020.105527.

[48] G. E. Hinton, "How neural networks learn from experience," 1992, pp. 145–151. https://doi.org/10.7551/mitpress/ 1888.003.0011.

[49] S. Altarazi, M. Ammouri, A. Hijazi, "Artificial neural network modeling to evaluate polyvinylchloride composites'

properties," Computational Materials Science, Vol. 153, 2018, pp. 1–9. https://doi.org/10.1016/j.commatsci.2018.06.003.

[50] M. M. Yadollahi, A. Benli, R. Demirbog˘a, "Prediction of compressive strength of geopolymer composites using anartificial neural network, "Materials Research Innovations, Vol. 19, No. 6, 2015, pp. 453–458. https://doi.org/10.1179/ 1433075X15Y.0000000020.

[51] G. V. Kumar, R. Pramod, C. S. P. Rao, P. S. Gouda, "Artificial neural network prediction on wear of Al6061 alloy metal matrix composites reinforced with-Al_2O_3," Materials Today: Proceedings, Vol. 5, No. 5, 2018, pp. 11268–11276. https://doi.org/10.1016/j.matpr.2018.02.093.

[52] R. Pramod, G. V. Kumar, P. S. Gouda, A. T. Mathew, "A study on the Al2O3 reinforced Al7075 metal matrix composites wear behavior using artificial neural networks," Materials Today: Proceedings, Vol. 5, No. 5, 2018, pp. 11376–11385. https://doi.org/10.1016/j.matpr.2018.02.105.

[53] K. M. Hossain, M. S. Anwar, S. G. Samani, "Regression and artificial neural network models for strength properties of engineered cementitious composites," Neural Computing and Applications, Vol. 29, 2018, pp. 631–645. https://doi.org/ 10.1007/s00521-016-2602-3.

[54] A. M. Hassan, A. Alrashdan, M. T. Hayajneh, A. T. Mayyas, "Prediction of density, porosity and hardness in aluminum–copper-based composite materials using artificial neural network," Journal of Materials Processing Technology, Vol. 209, No. 2, 2009, pp. 894–899. https://doi.org/10.1016/ j.jmatprotec.2008.02.066.

[55] A. Canakci, T. Varol, C. Nazik, "Effects of amount of methanol on characteristics of mechanically alloyed Al–Al2O3 composite powders," Materials Technology, Vol. 27, No. 4, 2012, pp. 320–327. https://doi.org/10.1179/17535557 12Y .0000000014.

[56] M.K. Kazi, F. Eljack, E. Mahdi, "Optimal filler content for cotton fiber/PP composite based on mechanical properties using artificial neural network," Composite Structures, Vol. 251, 2020, p. 112654. https://doi.org/10.1016/ j.compstruct. 2020.112654.

[57] M. Konieczny, "The effect of sintering temperature, sintering time and reinforcement particle size on properties of Al-Al2O3 composites," Composites Theory and Practice, Vol. 12, No. 1, 2012, pp. 39–43.

[58] M. Kargul, J. Borowiecka-Jamrozek, M. Konieczny, "The effect of reinforcement particle size on the properties of Cu-Al2O3 composites," in IOP Conference Series: Materials Science and Engineering, Vol. 461, No. 1, 2018, p. 012035. IOP Publishing. https://doi.org/10.1088/1757- 899X/461/ 1/012035.